Journal of the European Ceramic Society **11** (1993) 471–480

Relationships of Tetragonal Precipitate Statistics with Bulk Properties in Magnesia-Partially Stabilized Zirconia

Charles S. Montross*

Electron Microscope Center, University of Queensland, Queensland, Australia 4072

(Received 12 June 1992; revised version received 8 October 1992; accepted 28 October 1992)

Abstract

The toughness of magnesia-partially stabilized zirconia (Mg-PSZ) is controlled by metastable tetragonal precipitates that interact with crack tip stress fields. Understanding and controlling the precipitate size controls the resulting properties. The precipitate growth behaviour of Mg-PSZ (9·5 mol% MgO) samples was studied after an experimental regime of sintering, rapid quenching and isothermal aging at 1400°C and 1320°C. Average precipitate size on polished and etched samples was measured by SEM for each processing time and temperature. Precipitate sizes, precipitate population statistics, phase content of transformable tetragonal phase and fracture toughness are plotted and optimum precipitate sizes for maximum toughness are identified. Relationships between experimental results and martensitic theories are discussed. The precipitate population distributions did not follow those predicted by Lifshitz–Slyozov–Wagner-based theories.

Die Zähigkeit von Magnesium teilstabilisiertem Zirkoniumoxid (Mg-PSZ) wird von metastabilen tetragonalen Ausscheidungen bestimmt, die mit dem Spannungsfeld an der Rißspitze wechselwirken. Die resultierenden Eigenschaften des Materials werden von der Größe der Ausscheidungen bestimmt. Deshalb ist es wichtig zu verstehen, was ihre Größe bestimmen und wie sie eingestellt werden kann. Das Wachstumsverhalten der Ausscheidungen in Mg-PSZ (9·5 mol% MgO) Proben wurde untersucht, wobei die Probenherstellung durch Sintern, schnelles Abkühlen und anschließendes isothermisches Altern bei 1400°C und 1320°C erfolgte. Die mittlere Ausscheidungsgröße wurde an polierten und geätzten Proben mit Hilfe der SEM für jede Prozeßzeit und Temperatur bestimmt. Ausscheidungsgröße, Ausscheidungszahlstatistiken, Phasenanteil transformierbarer tetragonaler Phase und Bruchzähigkeit werden betrachtet und die optimale Ausschiedungsgröße für maximale Zähigkeit ermittelt. Die Beziehung zwischen den experimentellen Ergebnissen und martensitischen Umformungstheorie werden diskutiert. Die Ausscheidungszahlverteilungen folgten nicht den auf der Lifshitz–Slyozow–Wagner Theorie basierenden theoretischen Vorhersagen.

La ténacité des zircones partiellement stabilisées à la magnésie (Mg-PSZ) est contrôlée par des précipitations de phase quadratique métastables qui interagissent avec les champs de contraintes en front de fissure. La compréhension et le contrôle de la taille des précipitations est nécessaire pour prédire les propriétés résultantes. Le comportement à la croissance de précipités d'échantillons de Mg-PSZ (9·5 mol% MgO) a été étudié après un traitement expérimental de frittage, de trempe et de traitement isotherme à 1400 C et 1320 C. Une taille moyenne de précipitation a été mesurée par MEB sur des échantillons polis et attaqués, pour chaque condition de temps et de température. Les tailles des précipités, leur distribution, la teneur en phase quadratique transformable et la ténacité à la rupture sont présentées et les tailles optimales de précipité pour une ténacité maximale sont identifiées. Les relations entre les résultats expérimentaux et les théories de la transformation martensitiques sont discutées. Les distributions de taille de précipités ne suivent pas celles prédites par les théories de Lifshitz–Slyozov–Wagner.

1 Introduction

Zirconia ceramics have extensive industrial applications arising from various desirable chemical and physical characteristics. In particular, intense interest in zirconias was generated by the discovery in the late 1970s of their ability to retain a metastable tetragonal phase.[1–3] This metastable tetragonal

* Present address: National Chemical Laboratory for Industry (Kagaku Gijustu Kenkyusho), Tsukuba Research Center, 1-1 Higashi, Tsukuba, Ibaraki, 305 Japan.

Journal of the European Ceramic Society 0955-2219/93/$6.00

phase provided a means of enhancing the toughness of a zirconia ceramic to several times beyond that of untoughened ceramics. The metastability of the precipitates, and the resulting toughness, is regulated by both their size and size distribution. If the precipitate population is below a certain size, fracture-induced stress fields will not initiate transformation, and as a result no toughening occurs. If the precipitate population grows beyond a critical size, the cubic matrix and neighbouring precipitates will not provide enough elastic constraint and the tetragonal precipitates will spontaneously transform to the monoclinic phase upon cooling. Optimal properties may be achieved through either controlled cooling or quenching followed by isothermal aging, where precipitates are grown until the majority are contained within these two critical size limitations.[4] Precipitate size distributions will also have effects. If the size distribution is too broad, significant precipitate populations may exist that either will not toughen, being subcritical in size, or will have spontaneously transformed upon cooling, being overaged in size. Conversely, a very narrow size distribution may cause difficulty in controlling the population during heat treatment.

Studies of tetragonal precipitate formation focused initially on calcia-partially stabilized zirconia (Ca-PSZ), with the development of a thermal shock resistant calcia-partially stabilized zirconia refractory material.[5] The thermal shock resistance was due to the precipitation of a 0·1 μm monoclinic phase in cubic grains.[6,7] Analysis continued on the precipitation in both magnesia- and calcia-partially stabilized zirconia with crystallographic relations being developed.[8] The discovery of transformation toughening due to the retention of a metastable tetragonal phase[9] increased the interest in precipitation within zirconia bodies.[10–14] The optimum precipitate size for proeutectoid heat-treated Ca-PSZ and Mg-PSZ was reported to be approximately 0·1 μm and 0·2 μm, respectively, based on analysis of TEM micrographs. A more in-depth analysis was conducted on both Ca-PSZ and Mg-PSZ by Swain *et al.*[15] Based on TEM micrographs, the measured fracture toughness was plotted versus Ca-PSZ proeutectoid precipitate size with toughness reaching 6–9 MPa$\sqrt{\text{m}}$ for precipitates of approximately 0·1 μm in size. For the Mg-PSZ system, similar results were not yet considered possible by them. The Ca-PSZ system was not further developed due to the difficulty in obtaining optimal properties. This was due to a narrow critical size range.

Subsequent work in the Mg-PSZ system has included not only size versus aging, but has also emphasized the importance of precipitate size distribution.[4,16,17] Bateman *et al.*,[17] using TEM micrographs, analysed the precipitate population statistics using a large population sample at one temperature and time. None of these studies have considered correlations between average size and size distribution versus aging time at elevated temperatures. Furthermore, the size of precipitates which maximizes fracture toughness in Mg-PSZ based on a large population sample has not been noted. The temperature at which precipitation occurs also affects tetragonal metastability. Heat treatments on Mg-PSZ above the eutectoid temperature[11] in the cubic + tetragonal two-phase region (proeutectoid) and below the eutectoid temperature[18] in the tetragonal + MgO two-phase region (subeutectoid) are both reported to optimize mechanical properties.

Precipitate interaction or impingement was reported to affect the average growth rate in a poorly understood manner.[13,19–22] Hannink *et al.*,[13] based on TEM measurements of Ca-PSZ, plotted log (precipitate size) versus log (time) and noted a change in the growth exponent from 1/3 to 1/2. The initial growth exponent agreed with that predicted by the Lifshitz–Slyozov–Wagner (LSW)[23–25] theory. Marder *et al.*[20] later analysed the same system, plotted precipitate size versus $t^{1/3}$ for temperatures from 1000°C to 1400°C for several times less than 6 h and fitted lines to the data. No significant deviation from linearity was noted by them. Dickerson *et al.*[21] noted the 'rafting' of the precipitates (shown in Fig. A2 of Ref. 21) and that the impingement made size measurement difficult. They concluded that the interfacial reaction was the dominant mechanism with a precipitate growth exponent of 1/2 as compared to the 1/3 exponent noted by Hannink *et al.*[13] and Marder *et al.*[20] Hughan & Hannink[22] analysed the Mg-PSZ system and noted that the precipitates occur in clusters with the size changing and increasing as one progressed from the grain boundary towards the unreacted secondary precipitate zones, named by them as 'white spots'.

More recent work[19] investigated the growth of both pro- and subeutectoid tetragonal precipitates versus time at 1400°C and 1320°C, respectively. Based on the length measurements on their long ⟨100⟩ extension, the growth rate exponent matched that predicted for a volume diffusion-controlled growth mechanism by the LSW theory.[23–25] The coherency of the precipitates with the cubic matrix was also found to control the widthwise growth. A 1/5 growth exponent was found[19] which corresponds to growth across interfaces with boundary misorientation, mismatch, or low angle boundaries, which is not predicted by the LSW theories. The subeutectoid precipitate growth behaviour was similar to that reported by Hannink *et al.*[13] It was then initially assumed that the Mg-PSZ system obeyed the LSW model as had the Ca-PSZ system

been assumed to do.[13,20,21] Available time allowed additional investigation of the precipitation behaviour in Mg-PSZ by the author. Re-evaluation of the initial raw precipitate size data with regard to the precipitate population statistics identified that the behaviour did not match that predicted by LSW and that there was also a need for better statistics. This prompted the further investigation into the Mg-PSZ system as presented in this work.

The purpose of this research was to investigate several aspects of tetragonal precipitate growth in Mg-PSZ. The first was to analyse the precipitate population statistics with larger sample populations over larger areas than earlier analyses using scanning electron microscopy. These samples were measured as a function of time in both the pro- and subeutectoid temperature regions and the results compared with theory. The second was to verify, using the larger precipitate population samples, the effect of precipitate impingement on precipitate growth that was previously noted.[13,19-22] The third was to identify the precipitate size, both pro- and subeutectoid, which maximized the fracture toughness, K_{IC}, and phase content of transformable tetragonal phase. The fourth was to compare the predictions of the various theories on martensitic transformation and transformation toughening with experimental results.

2 Experimental Procedures

The 9·5 mol% MgO–90·5 mol% ZrO_2 Mg-PSZ composition was fabricated using high purity ZrO_2 (Z-Tech SF-Super Zirconia Powder, Z-Tech, Melbourne, Australia) powder ($SiO_2 < 80$ ppm) and MgO powder using procedures described elsewhere.[19] The samples were rapidly cooled from the 1700°C cubic solid-solution region sintering temperature to the isothermal hold temperatures of 1400°C and 1320°C and held for times of 0·25, 0·5, 1, 2, 5, 10 and 20 h, then rapidly cooled to room temperature. The rate of cooling exceeded 1000°C/h over the temperature range from 1700°C to approximately 900°C with rates of 3000°C/h achieved between 1700°C and 1400°C. The rapid cooling was used to prevent extraneous precipitate growth or phase changes as has been noted elsewhere.[26,27]

These samples were polished using 1 μm diamond paste and etched in concentrated HF acid. Such samples were prepared for and analysed by secondary electron microscopy and typical areas photographed. Printed micrographs were analysed for precipitate length with typically around 100+ precipitates measured per temperature and aging time. The average lengths and standard deviations were calculated. Automated image analysis systems had difficulty separating and analysing the tetragonal precipitates due to impingement. The precipitate length frequencies were normalized by dividing the number of precipitates per size range, or 'bucket', by the total number of precipitates measured. The number of 'buckets' per population sample was adjusted to clearly show the frequency behaviour. The normalized frequency is plotted versus size range or 'bucket' in Figs 1 and 2. The areas of the frequencies versus size curves were not normalized for samples of different times and temperatures.

The Vickers indentation method was used for measuring the room-temperature toughness as a function of aging time and temperature. Three indentations with 30 kg loads were used on each sample and the measured crack lengths and indentation diagonals averaged. The average indent diagonals and crack lengths were used to calculate the fracture toughness, K_{IC}. Several equations considered for use in this work included that proposed by Anstis *et al.*[28] and Evans & Charles.[29] These two methods were analysed and compared with a series of fracture toughness testing techniques by Stuart.[30] In Stuart's analysis, the equation of Evans & Charles[29] was found to give values closer to the true K_{IC}.

3 Results

3.1 Precipitate population statistics

Two typical normalized precipitate size population frequencies are plotted in Fig. 1 for samples aged for 0·25 and 0·5 h at 1400°C. The population distribution for precipitates aged for 0·25 h is skewed sharply to small sizes with a tail towards increasing sizes. For precipitates aged for 0·5 h, the distribution shifted to larger sizes as expected, remaining similar in shape though becoming broader.

For samples aged at 1320°C for times of 0·25 to 20 h, the normalized precipitate size population frequencies are plotted in Fig. 2. In all subeutectoid aged samples, no proeutectoid precipitates were

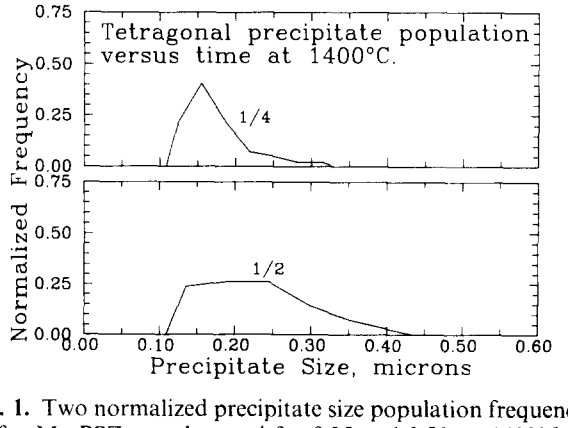

Fig. 1. Two normalized precipitate size population frequencies for Mg-PSZ samples aged for 0·25 and 0·5 h at 1400°C.

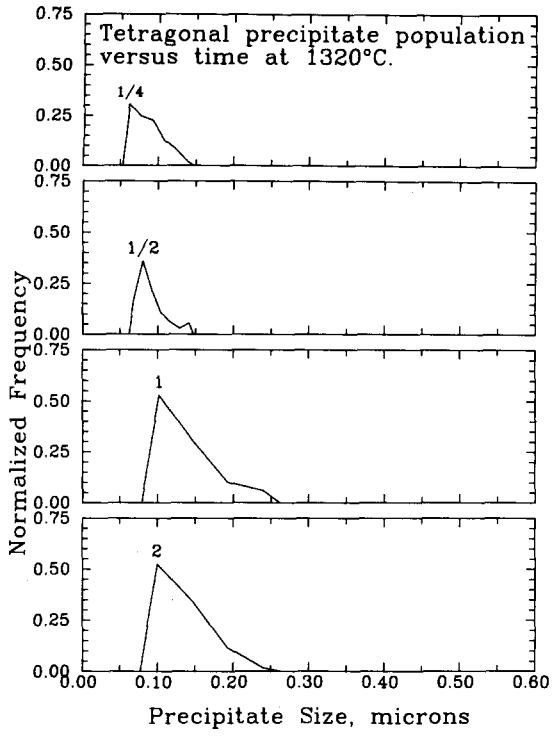

(a)

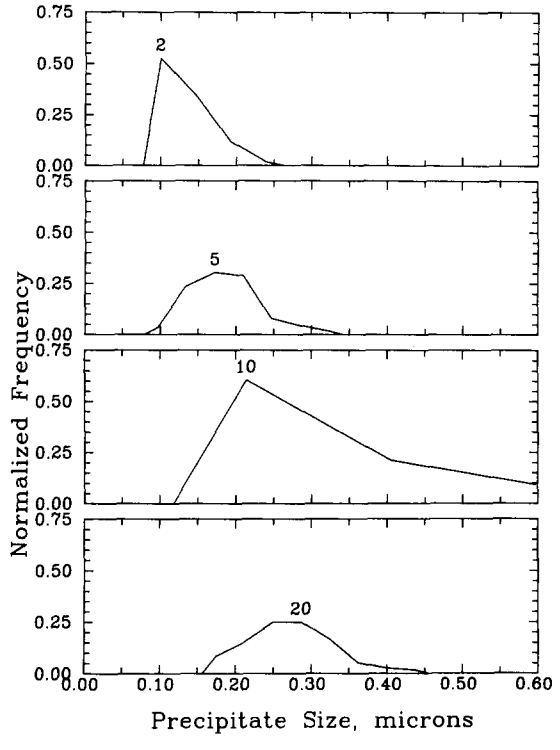

(b)

Fig. 2. Normalized precipitate size population frequencies for Mg-PSZ samples aged for (a) 0·25 to 2 h and (b) 2 to 20 h at 1320°C.

found, due to the rapid cooling from the cubic solid-solution temperature of 1700°C through the proeutectoid two-phase region to the subeutectoid isothermal aging temperature. Overall, the shape of the 1320°C population distributions are the same as the 1400°C distribution shapes. The population distributions for samples aged for 0·25 to 2 h are comparable to each other (Fig. 2(a)). For samples aged from 2 to 20 h, the population distributions (Fig. 2(b)) have a similar shape to samples that sustained shorter anneals, but the population distributions increase in breadth and the median values noticeably shift to larger sizes with increasing time. The subeutectoid sample aged for 10 h showed a large variation in precipitate sizes due to 'runaway' precipitate growth. Three micrographs were taken across the cubic grain in which the tetragonal phase precipitated. For this particular sample, 177 precipitates were measured in that grain to obtain the precipitate population statistics.

3.2 Precipitate size relationships

Average precipitate length and standard deviations at 1400°C are plotted in Fig. 3 and are shown to increase in size throughout the duration of the experiment. The slope of the resulting line is approximately 1/3, as measured by linear least squares analysis, which corresponds to the growth exponent.

The average precipitate length and the standard deviation when aged at 1320°C are plotted in Fig. 4. It had previously been noted and reported[13,19–22] that precipitate impingement affected precipitate growth. Precipitate impingement is expected to result in a change in growth behaviour and is indicated by changes in slope in precipitate length versus time. Preliminary results[19] indicated that precipitates grew rapidly from 1 to 2 h at 1320°C, then ceased to grow from 2 to 10 h. The present data derived from larger precipitate population samples using SEM micrographs indicate continuous precipitate growth, with a 1/3 exponent for all times at

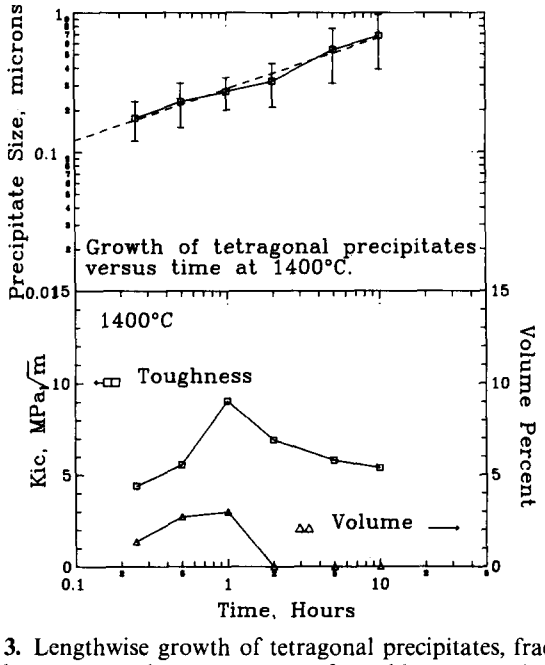

Fig. 3. Lengthwise growth of tetragonal precipitates, fracture toughness, K_{IC}, and percentage transformable tetragonal-phase content versus time at 1400°C.

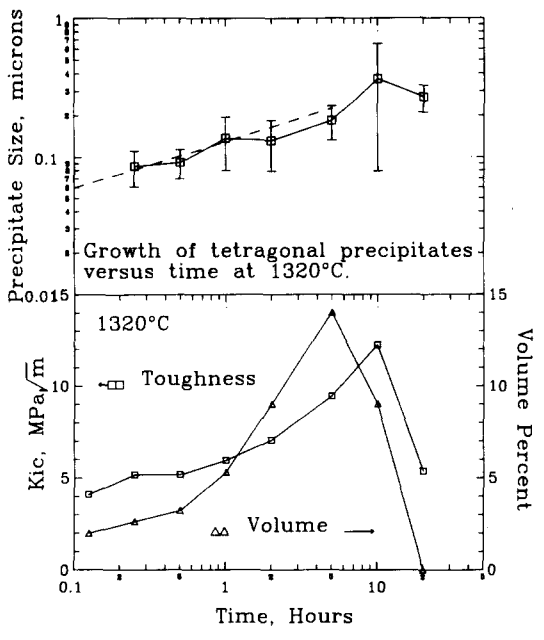

Fig. 4. Lengthwise growth of tetragonal precipitates, fracture toughness, K_{IC}, and percentage transformable tetragonal-phase content versus time at 1320°C.

this temperature. The necessity for large precipitate population samples may be appreciated by inspection of the precipitate size variations shown in a typical SEM micrograph, Fig. 5, of the sample aged at 1320°C for 10 h. For this specimen, a total of 177 precipitates were measured from three micrographs across the cubic grain to obtain the average length and standard deviation.

The larger precipitates seen in Fig. 5 are not of proeutectoid origin but are subeutectoid precipitates that experienced 'runaway' growth. Slow cooling rates of 500°C/h are known[22,31] to result in mixed populations of both pro- and subeutectoid precipitates. However, in this work, the cooling rate of 3000°C/h from 1700°C to 1400°C through the proeutectoid two-phase region would not have resulted in the growth of proeutectoid precipitates.

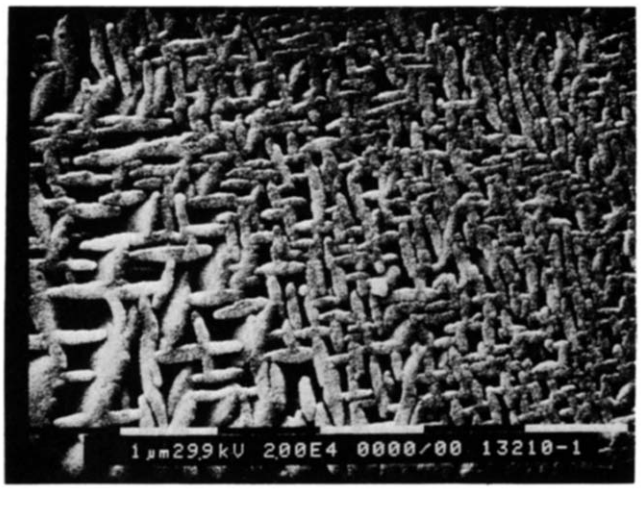

Fig. 5. SEM micrograph of the Mg-PSZ sample aged at 1320°C for 10 h showing typical tetragonal precipitate size variations.

Fast cooling rates of greater than 900°C/h have been shown not to change the phase content.[26,27] The variation in precipitate size in Fig. 5 was observed in other samples, but not to the same degree.

The measured phase content of the transformable tetragonal phase from previous work[19] for samples aged at both 1400°C and 1320°C is plotted in Figs 3 and 4, respectively. At the proeutectoid aging temperature 1400°C (Fig. 3) the transformable tetragonal-phase content was maximized at 3% after 1 h annealing. Rapid overaging occurred for longer annealing times as the precipitates exceeded the critical size. The measured fracture toughness peaked at 9·05 MPa$\sqrt{m}$ at 1 h in the 1400°C samples, coinciding with the highest transformable tetragonal-phase content, as shown in Fig. 3.

Subeutectoid aging at 1320°C (Fig. 4) resulted in a phase content of 14% by 5 h followed by a less rapid overaging. For the 1320°C samples, the maxima in tetragonal-phase content and toughness were not coincident, but temporally separated by 5 h. The maximum in toughness occurred at 10 h time with a value of 12·23 MPa$\sqrt{m}$, followed by a rapid decrease, as shown in Fig. 4.

For the 1400°C proeutectoid samples, the maximum toughness of 9·05 MPa$\sqrt{m}$, reached after 1 h, corresponds to an average precipitate size of approximately 0·3 μm (Fig. 3). With 1320°C subeutectoid annealed samples, the maximum transformable tetragonal-phase content (14%) was reached after 5 h aging and corresponds to an average precipitate size of just over 0·2 μm (Fig. 4). The maximum toughness of 12·23 MPa $\sqrt{m}$, occurring at 10 h time, corresponds to an average precipitate size of 0·3 μm. Despite the differences between pro- and subeutectoid tetragonal precipitates, it is notable that the same average precipitate size yields maximum toughness.

4 Discussion

4.1 Population statistics background and discussion

The basic assumptions underlying the Lifshitz, Slyozov & Wagner (LSW) theory are that precipitate growth is controlled by the degree of supersaturation with diffusion under steady-state conditions and no interaction between an infinitely dilute solution of second-phase particles of a constant volume fraction. The first stage of development consists of the growth of grains/precipitates directly from solution and continues until the degree of supersaturation has fallen such that growth stops. An additional assumption is that precipitation and coarsening occur sequentially and can be treated separately; this was considered reasonable by Lifshitz, Slyozov and Wagner for large precipitates.

Classically, growth kinetics and particle size distribution are related as follows:[23-25]

$$\frac{dr}{dt} = f(r,t)$$

$$\frac{dr}{dt} = \frac{K}{\gamma}\frac{1}{r^2} \qquad (1)$$

$$r^3 - r_0^3 = \frac{K}{\gamma}t$$

where K is a materials constant, γ is a numerical constant relating to particle size and time, r_0 is the critical precipitate radius at the onset of coarsening ($t=0$), and r is the observed radius. Much research and discussion has been conducted to develop a particle coarsening theory of a sophistication that not only permits the interpretation of experimental results, but also predicts grain growth in systems under various thermodynamic and kinetic regimes.

The constant, γ, was analysed[32-36] with respect to theoretical constraints and it was found that it could be varied and still meet the requirements of the LSW theory. Others analysed growth kinetics and particle size distribution with respect to mass transport, diffusion, particle constraint and diffusion geometries.[37-42] Tsumuraya & Miyata[41] developed six models meeting the $t^{1/3}$ law and accounted for several types of diffusion geometry controlled by precipitate spatial distributions and variable volume fractions of particles. Model III of Tsumuraya and Miyata considered a periodic array of separated precipitates in cubic directions to model the Ni(Al) and Ni(Cr, Al) systems. In model IV, the precipitates have the opportunity to contact each other. Bateman *et al.*[17] considered Model III to be the closest to their PSZ data. However, all the models of Tsumuraya & Miyata have precipitate sizes skewed to larger sizes.

Pande and coworker[43-45] treated grain growth as a statistical or stochastic process. The rate equation used by Pande and coworker is the Langevin equation (eqn (2)), which has a deterministic term and a fluctuation term:

$$\frac{dR}{dt} = f(R,t) + T(t) \qquad (2)$$

The deterministic term, $f(R,t)$, is based on the curvature and controlled migration of the grain boundary. The stochastic term, $T(t)$, is noise due to connected grain boundary motion and motion directed by surface tension forces. This was applied to a one-dimensional Fokker–Planck second-order partial differential equation for grain growth size distributions. The solution is a size distribution based on a degenerate hypergeometric function defined by a series that has a form similar to a log normal distribution. The equations used and the resulting distribution, F, are shown below:

$$f(R,t) = \alpha\left(\frac{1}{R_c} - \frac{1}{R}\right)$$

$$\alpha = \alpha_0\mu_0\gamma$$

$$\frac{\partial F}{\partial t} = -\frac{\partial}{\partial R}\left[\left(\frac{\alpha}{R_c} - \frac{\alpha}{R}\right)\right]F + \frac{D}{2}\frac{\partial^2 F}{\partial R^2} \qquad (3)$$

$$F = \frac{\text{Constant}}{t^{3/2}} R\left[\Phi\left(\frac{3}{2}, \frac{\alpha}{D} + \frac{3}{2}; \frac{-R^2}{2Dt}\right)\right]$$

where

$$\Phi(A,B;Z) = 1 + \frac{AZ}{B1!} + \frac{A(A+1)Z^2}{B(B+1)2!} + \frac{A(A+1)(A+2)Z^3}{B(B+1)(B+2)3!} + \cdots$$

where R_c is the critical grain size, α_0 is a geometric factor, μ_0 is the grain boundary mobility, γ is the surface energy, and D is the diffusion constant. D is considered to be a scaling factor for the time variable which agrees with experiments. The term α/D determines the proportion of the deterministic (α) to random components (D). When $\alpha/D = 0$, the classical Rayleigh distribution in one dimension results. T, the 'noise' or stochastic term, was not found to improve agreement with experiments.

Pande & Dantsker[45] further develop the theory with an N-dimensional term, where N is the number of dimensions. For $N=3$, volume is strictly conserved. The grain size distribution for $N=3$ is obtained in close analytical form similar to the result in eqn (3), and is found to be approximate to a log normal distribution. They compared the resulting one- and three-dimensional grain size distributions. With increasing α/D (decreasing random component (D)), the one- and three-dimensional distributions become similar. They also compared the three-dimensional and log normal distributions which increase in similarity with a decreasing random component. In their conclusion, they state that the stochastic nature of grain growth is supported by available experimental, computer and theoretical calculations. Their one- and three-dimensional functions have distributions skewed to small sizes, similar to that observed for Mg-PSZ.

Evans *et al.*[46] analysed the martensitic transformation in zirconia ceramics based on energy changes and particle size effects. Martensitic transformation results in large shear strains with no significant macroscopic shear. The transformed particles consist of a series of sheared plates in which alternate plates have experienced shear deformation of opposite sign. The energy changes attributed to the twinned structure of martensite are considered to be the source of the transformation size effect. The

strain energy associated with twinning is more closely related to the surface area of the particles. The spacing between twinned plates is assumed to be approximately independent of particle size and is consistent with experimental results obtained with Fe particles precipitated in a Cu/Fe system and with zirconia.

Based on the energy changes, Evans *et al.* calculated the relative toughness, Γ_t/Γ_0, where Γ_t is the toughening increment and Γ_0 is the intrinsic toughness, using a uniform particle size distribution:

$$\frac{\Gamma_t}{\Gamma_0} = \frac{1}{1-\zeta} \qquad \zeta = f(V_f, \Delta V, \gamma_T, \eta_c, \omega) \tag{4}$$

where V_f is volume fraction of particles, ΔV is change in volume due to transformation, γ_T is the twin surface energy, η_c is the critical number of twins in a particle, and ω is a relaxation parameter. Significant deviations can be expected when a size distribution of particles exists. Evans *et al.* assumed an extreme value function of the particle size distribution where:

$$\Phi(a)\,da = k\frac{a_0^k}{a^{k+1}}\exp\left[-\left(\frac{a_0}{a}\right)^k\right]da \tag{5}$$

and where a_0 is the scale parameter, d is the twin spacing and k is the shape parameter. The ζ then changes to yield:

$$\zeta = f\left(V_f, \Delta V, \gamma_T, \eta_c, \omega, I\left(\frac{a}{a_c}, k\right)\right)$$

where

$$I\left(\frac{a}{a_c}, k\right) = \int_0^{a_c} a^3 \frac{(2{\cdot}4d + a)}{(a_c - a)} \left[k\frac{a_0^k}{a^{k+1}}\exp -\left(\frac{a_0}{a}\right)^k\right]da \tag{6}$$

The predicted relative toughening was plotted as a function of particle size for several values of k ($k = 4$, 7, 10) in Fig. 6 of Ref. 46. The distribution is skewed to smaller sizes similar to the log normal distribution. The relative toughness was compared to the relative particle size with respect to toughness data for some PSZ materials. A particle shape parameter of $k = 6$ was reported to best fit the data used. The model was then applied to data obtained for the Al_2O_3/ZrO_2 system where relative toughness was plotted versus volume fraction of zirconia. The model predictions, where the shape factor $k = 7$, was shown to approximate the data presented. The chosen population distribution function, the extreme value function, results in the model matching the experimental results.

The selection of the extreme value function for the particle size distribution was based on research experience[47] from the toughening of ceramics by circumferential microcracking around second-phase particles. Evans & Faber[47] noted that the major contribution to toughening occurs from particles just below the critical size. Particles equal to or greater than the critical size would have microcracked spontaneously. An extreme value function was selected by Evans & Faber[47] to produce a large population of unmicrocracked particles to result in the highest toughness. This same extreme value function was selected for use in the martensitic transformation analysis for similar reasons. This distribution function, also similar to the log normal function, fortuitously matches the population data presented in this research paper. Closer inspection of Fig. 4 of Ref. 17 also reveals that the size frequency versus l/l_{ave} is skewed to smaller sizes. There is a tail extending to large sizes, ending at 2·1 l/l_{ave}, and a sharp increase in size frequency at small sizes, beginning at 0·4 l/l_{ave}.

4.2 Martensitic transformation theory and discussion

With respect to Mg-PSZ, several complex reactions and events occur during precipitation and growth, which is also dependent upon temperature of precipitation. The differences in maximum toughness values are postulated to be due to two independent causes: the amount of MgO in solution in the precipitates and differences in martensitic embryo populations.

According to the MgO–ZrO_2 phase diagram,[48] in the proeutectoid cubic + tetragonal two-phase field, MgO remains in solution in both phases. In the subeutectoid region, the MgO comes out of solution to form the tetragonal zirconia + MgO two-phase field. As the subeutectoid precipitates form and/or grow, MgO is forced into the 'white spots', increasing the concentration of MgO there.[49,50] 'White spots' is the term given[22,31] to the highly reflective regions in etched subeutectoid aged specimens and are due to the reflective difference between etched proeutectoid cubic or cubic + tetragonal phases and the subeutectoid precipitates. These 'white spots' are formed by the heterogeneous nucleation of subeutectoid precipitates that propagate into the grain from the grain boundary. The exosolution of MgO from the precipitates at 1320°C results in a higher phase content of transformable tetragonal phase and a higher toughness value as seen from comparing Figs 3 and 4. The average precipitate size for maximum fracture toughness is the same for both temperatures, 0·3 μm. This follows the theory proposed by Lange & Green[51] for critical size effects on precipitates in transformation-toughened ceramics. In their paper, they present data for the effect of yttria content on critical grain size for retention of a

metastable tetragonal phase. Decreasing stabilizer content results in a decreasing critical size for metastable tetragonal grains. This is also noted by Claussen & Rühle,[52] where chemical alloying affects the toughening potential of the metastable tetragonal phase. In summary, at constant precipitate size, the more the stabilizer content decreases, the more the metastability of the tetragonal phase increases and the more readily it will transform.

Based on metallic systems, several investigators consider that martensite grows from preexisting embryos.[53,54] These embryos are thought to consist of an intermediate structure between the two phases (metastable and stable) and are formed by faulted structures such as dislocations or stacking faults. Andersson & Gupta[55] consider the nature of preexisting embryos to be unknown in partially stabilized zirconias. Kaufman & Cohen[56] note that embryos could be formed at higher temperatures by thermal activation and frozen in as the temperature is lowered. One possible source of these martensite embryos could be the interface of the c axis of the tetragonal precipitate with the cubic matrix, which exhibited growth corresponding to interfaces with boundary misorientation, mismatch or low angle boundaries.[19] TEM analysis of the proeutectoid precipitates by Heuer[57] showed coherent interfaces and he noted that incoherent interfaces would be desirable for transformation to occur readily. The coherency of the interface affects the Helmholtz free energy for transformation, since the martensitic nucleation will be difficult until the interface becomes semi- or incoherent.

Another possible source of martensitic embryos could be due to fault structures in untransformed metastable subeutectoid precipitates formed by neighbouring, overaged, transformed subeutectoid precipitates. This can be seen by comparing the average precipitate size for maximum transformable tetragonal phase content with the average size for maximum fracture toughness. In Fig. 4 for subeutectoid aged samples, these two precipitate sizes are not the same. A precipitate size of 0·2 μm yields a maximum in transformable tetragonal-phase content of 14%. A further 5 h isothermal aging results in a decrease to 9% transformable phase content, but an increase in toughness to a maximum of 12 MPa$\sqrt{\text{m}}$. When the precipitates overaged, there was an increase of 5% in the polished monoclinic phase content.

The increase in spontaneously transformed overaged precipitates is hypothesized to cause the formation of martensitic nuclei in the remaining untransformed precipitates. The impingement of the precipitates also facilitates nuclei formation, since the long axis of each precipitate is in contact with the neighbouring precipitate's surface with boundary mismatch. When the overaged precipitates spontaneously transform, martensitic nuclei are expected to have formed in the impinged precipitates. A small population should be sufficient to produce a larger population with martensitic nuclei.

5 Conclusions

(A) The maximum toughness reached with the 1400°C aged samples was 9 MPa$\sqrt{\text{m}}$, coinciding with the maximum in transformable tetragonal phase content of 3%. The optimum precipitate size for maximum toughness was measured to be 0·3 μm.

(B) For the 1320°C aged samples, the maximum in transformable tetragonal-phase content did not coincide temporally with the maximum in toughness by 5 h aging time. The optimum precipitate size for the maximum transformable tetragonal phase content of 14% was measured to be just over 0·2 μm.

(C) For the 1320°C aged samples, the maximum in toughness of 12·2 MPa$\sqrt{\text{m}}$ had an optimum precipitate size of 0·3 μm. The optimum precipitate size for maximum toughness was the same for both 1400°C and 1320°C aged samples.

(D) The differences in maximum toughness values is postulated to be due to two causes: the solution of MgO in the precipitate, and the population of martensitic nuclei. The solubility of MgO is very low in the subeutectoid precipitates, as compared to the proeutectoid precipitates. The subeutectoid precipitate population was slightly overaged by 5 h at the maximum in fracture toughness, with a decrease in transformable tetragonal phase content from 14 to 9%. The impingement of the overaged transformed tetragonal precipitates is hypothesized to result in the formation of martensitic nuclei in neighbouring precipitates.

(E) Precipitate impingement did not have an effect on the precipitate growth exponent as noted in previous literature. The larger population, measured from SEM micrographs, used in this work for statistical measurements eliminated reported changes in growth behaviour.

(F) The precipitate size distributions for samples aged at 1400°C were skewed to small sizes. The precipitate size distributions for samples aged at 1320°C were also skewed to small sizes. This skewness existed even though there was a variation of precipitate sizes due to 'runaway' growth.

(G) The precipitate size distribution predicted by the Lifshitz, Slyozov and Wagner (LSW) theories did not match the experimental distribution. The LSW size distribution is skewed to larger precipitate sizes. There are two theories that came closest to matching the observed size distribution skewed to smaller sizes: the one proposed by Pande and coworker and the one proposed by Evans *et al.* The theory of Pande and coworker using stochastical processes and strong deterministic growth component, has a distribution skewed to small sizes, similar to that observed for Mg-PSZ. The theory of Evans *et al.* relates martensitic transformation energies and experimental results to a particle size distribution based on the extreme value function. Appropriate selection of the shape parameter results in experimental results matching theoretical predictions. The resulting particle size distribution also matches the experimental size distribution shown in this work.

Acknowledgements

The author would like to express his appreciation to the Australian Industrial Research and Development Board for the funding for this research through grant number 15010 to Dr Ian Mackinnon of the Electron Microscope Center at the University of Queensland, Australia. Drs I. Mackinnon, T. White, H. Yokokawa and B. van Hassel are thanked for their comments during the writing of this paper.

References

1. Gupta, T. K., Bechtold, J. H., Kuznicki, J. H. & Rossing, B. R., *J. Mater. Sci.*, **12** (1977) 2421–6.
2. Gupta, T. K., Lange, F. F. & Bechtold, J. H., *J. Mater. Sci.*, **13** (1978) 1464–70.
3. Pascoe, R. T., Hannink, R. H. J. & Garvie, R. C., *Sci. Ceram.*, **9** (1977) 447.
4. Green, D. J., Hannink, R. H. J. & Swain, M. V., *Transformation Toughening of Ceramics*. CRC Press, Boca Raton, FL, 1989, pp. 98–103.
5. Garvie, R. C., Partially stabilized zirconia refractory. US Patent 3,620,781, 16 November 1971.
6. Garvie, R. C. & Nicholson, P. S., *J. Amer. Ceram. Soc.*, **55**(3) (1972) 152–7.
7. Green, D. J., Maki, D. R. & Nicholson, P. S., *J. Amer. Ceram. Soc.*, **57**(3) (1974) 136–9.
8. Bansal, G. K. & Heuer, A. H., *J. Amer. Ceram. Soc.*, **58**(5–6) (1975) 235–8.
9. Garvie, R. C., Hannick, R. H. J. & Pascoe, R. T., *Nature (London)*, **258** (5537) (1975) 703–4.
10. Porter, D. L. & Heuer, A. H., *J. Amer. Ceram. Soc.*, **60**(3–4) (1977) 183–4.
11. Porter, D. L. & Heuer, A. H., *J. Amer. Ceram. Soc.*, **62**(5–6) (1979) 298–305.
12. Schoenlein, L. H. & Heuer, A. H., In *Fracture Mechanics of Ceramics*, Vol. 6, ed. R. C. Bradt, A. G. Evans, D. P. H. Hasselman & F. F. Lange. Plenum Press, New York, 1983, pp. 309–26.
13. Hannink, R. H. J., Johnston, K. A., Pascoe, R. T. & Garvie, R. C., In *Advances in Ceramics*, Vol. 3, ed. A. H. Heuer & L. W. Hobbs. American Ceramic Society, Westerville, OH, 1981, pp. 116–36.
14. Heuer, A. H., In *Advances in Ceramics*, Vol. 3, ed. A. H. Heuer & L. W. Hobbs. American Ceramic Society, Westerville, OH, 1981, pp. 98–115.
15. Swain, M. V., Hannick, R. H. J. & Garvie, R. C., In *Fracture Mechanics of Ceramics*, Vol. 6, ed. R. C. Bradt, A. G. Evans, D. P. H. Hasselman & F. F. Lange. Plenum Press, New York, 1983, pp. 339–54.
16. Jun-ichi Echigoya, Kiyotaka Sasai & Hajime Suto, *Trans. Japan. Inst. Metals*, **29**(7) (1988) 561–9.
17. Bateman, C. A., Notis, M. R. & Williams, D. B., *J. Amer. Ceram. Soc.*, **72**(12) (1989) 2372–6.
18. Hannink, R. H. J. & Swain, M. V., *J. Aust. Ceram. Soc.*, **18**(2) (1982) 53–62.
19. Montross, C. S., In *Proc. Int. Ceram. Conf., Aust. Ceram. 90* Perth, August 1990, ed. P. J. Darragh & R. J. Stead. TransTech Publications Ltd, Aedermannsdorf, Switzerland, pp. 772–7.
20. Marder, J. M., Mitchell, T. E. & Heuer, A. H., *Acta Metall.*, **31**(3) (1983) 387–95.
21. Dickerson, R. M., Swain, M. V. & Heuer, A. H., *J. Amer. Ceram. Soc.*, **70**(1) (1987) 214–16.
22. Hughan, R. R. & Hannink, R. H. J., *J. Amer. Ceram. Soc.*, **67**(7) (1986) 556–63.
23. Greenwood, G. W., *Acta Metall.*, **4** (1956) 243–8.
24. Lifshitz, I. M. & Slyozov, V. V., *J. Phys. Chem. Solids*, English translation, Pergamon Press, **19** (1–2).
25. Wagner, C., *Z. Elektrochem.*, **65**(7–8) (1961) 581–91.
26. Nettleship, I. & Stevens, R., *Brit. Ceram. Trans. J.*, **86** (1987) 183–6.
27. Montross, C. S., *J. Amer. Ceram. Soc.*, **73**(2) (1992) 463–8.
28. Anstis, G. R., Chantikul, P., Lawn, B. R. & Marshall, D. B., *J. Amer. Ceram. Soc.*, **64**(9) 1981) 533–43.
29. Evans, A. G. & Charles, E. A., *J. Amer. Ceram. Soc.*, **59**(7–8) (1976) 371–2.
30. Stuart, M. D., *Mater. Sci. Forum*, **34–36** (1988) 123–8.
31. Hannink, R. H. J. & Lowe, B. J., In *Proc. 12th Australian Ceramics Conf.*, Australian Ceramic Society, Melbourne, Australia, 1986, pp. 155–62.
32. Hoyt, J. J., *Scripta Metall. Mater.*, **24**(1) (1990) 163–6.
33. Brown, L. C., *Scripta Metall. Mater.*, **24**(11) (1990) 2231–4.
34. Brown, L. C., *Acta Metall. Mater.*, **37**(1) (1989) 71–7.
35. Brown, L. C., *Scripta Metall. Mater.*, **25**(1) (1991) 261–4.
36. Marqusee, J. A. & Ross, J., *J. Chem. Phys.*, **79** (1983) 373.
37. Ardell, A. J., *Acta Metall.*, **21**(1) (1972) 61.
38. Hillert, M., Hunderi, O., Ryan, N. & Saitre, T. O., *Scripta Metall.*, **23**(10) (1989) 1979–82.
39. Rios, P. R., *Acta Metall. Mater.*, **38**(10) (1990) 2017–21.
40. Miyazaki, T. & Doi, M., *Mater. Sci. Engng*, **A110** (1989) 175–85.
41. Tsumuraya, K. & Miyata, Y., *Acta Metall.*, **31**(3) (1983) 437–52.
42. Jayanth, C. S. & Nash, P., *J. Mater. Sci.*, **24** (1989) 3041–52.
43. Pande, C. S., *Acta Metall.*, **35** (1987) 2671–6.
44. Pande, C. S. & Dantsker, E., *Acta Metall. Mater.*, **38**(6) (1990) 945–51.
45. Pande, C. S. & Dantsker, E., *Acta Metall. Mater.*, **39**(6) (1991) 1359–65.
46. Evans, A. G., Burlingame, N., Drory, M. & Kriven, W. M., *Acta Metall.*, **29** (1981) 447–56.
47. Evans, A. G. & Faber, K. T., *J. Amer. Ceram. Soc.*, **64**(7) (1981) 394–8.
48. Grain, C. F., *J. Amer. Ceram. Soc.*, **50**(6) (1967) 288–90.
49. Nairn, J. & St John, D. H., *Mater. Sci. Forum.*, **34–36** (1988) 111–15.
50. Hay, S., Nairn, J. & St John, D. H., In *Proc. Int. Ceram.*

Conf., Aust Ceram 90, Perth, August 1990, ed. P. J. Darragh & R. J. Stead. Trans Tech Publications, Ltd Aedermannsdorf, Switzerland, pp. 744–9.
51. Lange, F. F. & Green, D. J., In *Advances in Ceramics*, Vol. 3, ed. A. H. Heuer & L. W. Hobbs. American Ceramic Society, Westerville, OH, 1981, pp. 217–25.
52. Claussen, N. & Rühle, M., In *Advances in Ceramics*, Vol. 3, ed. A. H. Heuer & L. W. Hobbs. American Ceramic Society, Westerville, OH, 1981, pp. 137–63.
53. Knapp, H. & Dehlinger, V., *Acta Metall.*, **4** (1956) 289–94.
54. Olsen, G. B. & Cohen, M., (I) *Metall. Trans. A.*, **7** (1976) 1897–904; (II) *Metall. Trans. A.*, **7** (1976) 1904–14; (III) *Metall. Trans. A*, **7** (1976) 1915–23.
55. Andersson, C. A. & Gupta, T. K., In *Advances in Ceramics*, Vol. 3, ed. A. H. Heuer & L. W. Hobbs. American Ceramic Society, Westerville, OH, 1981, pp. 184–201.
56. Kaufman, L. & Cohen, M., In *Progress in Metal Physics*, Vol. 7, ed. B. Chalmers & R. King. Pergamon Press, London, 1958, pp. 165–246.
57. Heuer, A. H., In *Advances in Ceramics*, Vol. 3, ed. A. H. Heuer & L. W. Hobbs. American Ceramic Society, Westerville, OH, 1981, pp. 98–115.